

PACS 61.05.cp, 61.43.Fs, 61.80.Ed

Radiation/annealing-induced structural changes in $\text{Ge}_x\text{As}_{40-x}\text{S}_{60}$ glasses as revealed from high-energy synchrotron X-ray diffraction measurements

T.S. Kavetsky¹, V.M. Tsmots¹, A.L. Stepanov^{2,3}

¹*Ivan Franko Drohobych State Pedagogical University,
Solid-State Microelectronics Laboratory,*

24, I. Franko str., 82100 Drohobych, Ukraine

²*Kazan Physical-Technical Institute, Russian Academy of Sciences,
10/7 Sibirskiy trakt, 420029 Kazan, Russian Federation*

³*Kazan Federal University, 18, Kremlyovskaya str., 420008 Kazan, Russian Federation*

Abstract. Local atomic structure of $\text{Ge}_x\text{As}_{40-x}\text{S}_{60}$ glasses ($x = 16, 24, 32,$ and 36) has been investigated in the γ -irradiated (2.41 MGy dose) and annealed after γ -irradiation states by using the high-energy synchrotron X-ray diffraction technique. The accumulated dose of 2.41 MGy is chosen to be close to the known in literature focal point (~ 2.0 MGy) for the system tested, at which the γ -irradiation-induced optical (darkening) effect does not depend on the composition. It is established that the first sharp diffraction peak (FSDP) is located at around 1.1E^{-1} in the structure factors $S(Q)$ of all the alloys studied. The FSDP position is found to be constant on radiation/annealing treatment, but the intensity of the FSDP reveals changes under irradiation/annealing only for the compositions with $x = 16$ and 24 . The radiation/annealing-induced changes are also observed on the pair distribution functions in the first and second coordination shells for these compounds. Practically invisible effects on the FSDP and pair distribution functions are found for the alloys with $x = 32$ and 36 . The radiation/annealing-induced structural changes detected mainly in the As–S sub-system of the glasses examined are well explainable within the Tanaka approach for interpretation of the photo-induced structural changes and related phenomena in As_2S_3 chalcogenide glass and similar materials.

Keywords: chalcogenide glasses, structure, X-ray diffraction, radiation modification.

Manuscript received 20.06.12; revised version received 15.08.12; accepted for publication 17.10.12; published online 12.12.12.

1. Introduction

The concept of coordination defects or valence alternation pairs (VAPs) in chalcogenide glasses is a fundamental and topical problem for understanding the structure and properties of these materials. Nevertheless, there are a lot of contradictions between researches in application of the VAP concept for explanation of different processes and phenomena in chalcogenide glasses. For instance, Dembovskii *et al.* [1] showed that the generally accepted concept of VAPs must be

reexamined, since formation of pairs of separated charged point defects of the type C_3^+ and C_1^- requires too much energy. On the other hand, the authors have shown by analogy with α -Se that centers connected by a strong bond can coexist in the form of rigid VAP dipoles. It was also found in [1] that nonrigid, metastable, hypervalent configurations (HVCs) exist in the form of HVC dipoles, which are neutral and diamagnetic in the ground state and lie below C_1^0 on the energy scale.

Recently, Munzar and Tichy [2] have reported that kinetics of photo-darkening of amorphous As_2S_3 and $a\text{-As}_2\text{Se}_3$ thin films follows a single exponential, but the magnitude and the rate of the process is higher in the case of As_2S_3 . The authors found out explanation for these facts estimating the probability of breaking of As–S and As–Se bonds on illumination. They showed that in the case of $a\text{-As}_2\text{S}_3$ around two bonds can be broken from each 2000 As–S bonds, whereas in the case of $a\text{-As}_2\text{Se}_3$ around two bonds can be broken only for each 10^8 As–Se bonds. It means the probability of photo-induced bond breaking in $a\text{-As}_2\text{S}_3$ film is much higher than that for $a\text{-As}_2\text{Se}_3$ film. As a result, it has been concluded in [2] that photo-darkening in $a\text{-As}_2\text{S}_3$ is accompanied by changes in short-range order interactions, while photo-darkening in $a\text{-As}_2\text{Se}_3$ is accompanied rather by changes in Coulomb interactions in an agreement with “slip motion of the layers” model introduced by Shimakawa *et al.* [3]. The estimated probability for $a\text{-As}_2\text{S}_3$ corresponds to the existence of concentration of defects at the level less than 1% of all atomic sites. Is this level of concentration of defects enough to be identified using a experimental technique like X-ray diffraction (XRD), which can provide direct structural information?

Tanaka [4] mentioned that reversible photo-induced phenomena, involving structural changes at atomic sites of 10^{17} – 10^{18}cm^{-3} (approximately ppm order [5]), exist in tetrahedral and chalcogenide systems. The density is comparable to that of point defects in crystals, and it is far below a detection limit of the XRD technique. Thus, mechanisms of these phenomena are largely speculative, especially, when related sites are ESR-inactive. However, there are several photo-induced phenomena involving atomic sites of ~1% [5] and these kinds of phenomena have only been detected for chalcogenide glasses. If considering all the photo-induced phenomena (see Table 1 in [4]) involving atomic sites less and more than $\sim 10^{20}\text{cm}^{-3}$ or ~1% of the total atom density, these phenomena can be both irreversible and reversible. The irreversible phenomena can involve greater atom numbers, since the changes occur towards more stable atomic structures (see Table 1 in [4]); then, why should the atomic sites be less than 1% in the reversible changes according to the Tanaka model? This fact is considered [4] as follows: “*The density of 1% reads one photo-induced atomic site per cube with a side length of 5-6 atoms, which is 1-3 nm, depending on the atomic bonds involved, i.e. covalent and/or van der Waals bonds. The atomic density of defects 1% is the limit arising from the structures that can localize photo-induced strains. The critical length of 1-3 nm is comparable to the medium-range structural length in chalcogenide glasses*”. According to the Tanaka model, the photo-structural changes on the medium-range order scale may be considered as a signature of photo-induced defect formation with the density less than 1%

per cube with a side length of 5-6 atoms (1-3 nm). This is indeed observed [4] in the case of bulk glass As_2S_3 using the XRD method (the medium-range order is exemplified by the first sharp diffraction peak (FSDP)). The photo-structural changes may be explained in terms of defect models, presuming creation of some kinds of defects, and a non-defect or distortion model, postulating randomness increase in normal bonding configurations; although structural changes interpreted within the distortion model appear to be consistent with experimental observation of the FSDP weakening and broadening on illumination [4].

In contrast to the intensive study of photo-structural changes in chalcogenide glasses using the XRD method, less information and lack of our knowledge to understand γ -irradiation-induced structural changes in these materials are available, although, there are some methodological advantages to XRD study of γ -irradiation-induced effects as compared to the photo-induced ones. First, in the case of photo-induced phenomena [4], illumination and diffraction measurements should be performed *in-situ*, which is important to exclude thermal expansion effects and to detect minute changes. While for radiation-induced phenomena, γ -irradiation produces changes inside the whole glass matrix, but not in the spot as for laser illumination, and, thus, an *in-situ* experiment is not required and it is not possible to be performed experimentally in the case of γ -irradiation. Second, the investigation of radiation-modified structure of a glass is important within *ex-situ* measurements in order to find how structure is changed after a long period of time following radiation treatment of a sample (static radiation-induced effects [6–8]). Third, in contrast to photo-induced phenomena (irreversible or reversible), γ -irradiation-induced phenomena are mainly always reversible with annealing at the temperature 40-50 K below the glass transition temperature T_g [9, 10], which allows to investigate the radiation/annealing-induced structural changes for the same sample measured first as γ -irradiated and then as annealed after γ -irradiation under the same experimental conditions.

The purpose of this work is to study the radiation/annealing-induced structural changes in $\text{Ge}_x\text{As}_{40-x}\text{S}_{60}$ ($x = 16, 24, 32, \text{ and } 36$) glasses using the high-energy synchrotron XRD technique. Among a number of chalcogenides, as far as we know, only this system demonstrates the focal point (~ 2.0 MGy), at which the γ -irradiation-induced optical (darkening) effect does not depend on the composition [11]. We believe that the glasses examined should also exhibit this effect at the accumulated dose close to 2.0 MGy. The origin of the focal point is not clear, and we suggest that the precise high-energy synchrotron XRD study of the $\text{Ge}_x\text{As}_{40-x}\text{S}_{60}$ glasses in the γ -irradiated and annealed after γ -irradiation states under the same experimental conditions will help us to obtain more information and to cast light on this issue.

2. Experimental

The bulk glasses of $\text{Ge}_x\text{As}_{40-x}\text{S}_{60}$ system at $x = 16, 24, 32,$ and 36 were prepared from elements of 99.9999% purity in evacuated silica ampoules by standard melt quenching procedure as described elsewhere [12]. As-prepared glasses were cut to the disk-like specimens and polished to a high optical quality. Then, in order to remove possible mechanical stresses formed after synthesis, the samples were annealed at about 20-30 K below the glass transition temperature [12] ($T_g = 530$ K for $\text{Ge}_{16}\text{As}_{24}\text{S}_{60}$, 620 K for $\text{Ge}_{24}\text{As}_{16}\text{S}_{60}$, 670-675 K for $\text{Ge}_{32}\text{As}_8\text{S}_{60}$, and 682 K for $\text{Ge}_{36}\text{As}_4\text{S}_{60}$).

Radiation treatment of the glasses was performed by γ -quanta (average energy $E = 1.25$ MeV) with the accumulated dose 2.41 MGy (close to the focal point [11] near 2.0 MGy) at normal conditions of stationary radiation field created in a closed cylindrical cavity by a number of circularly established ^{60}Co radioisotope capsules. No special measures were taken to prevent uncontrolled thermal annealing of the samples, but maximum temperature in the irradiating camera did not exceed 320-330 K during prolonged γ -irradiation (about 30 days), providing the absorbed dose power $P < 5$ Gy/s. The γ -irradiated samples were measured for more than 2 months after γ -irradiation (static component of radiation-induced effects [6-8]). The γ -irradiated samples were annealed at the temperature 40-50 K below T_g following the previous results on the reversible γ -irradiation-induced optical (darkening) effects in the $\text{Ge}_x\text{As}_{40-x}\text{S}_{60}$ glasses with thermal annealing [9, 10].

High-energy synchrotron X-ray diffraction experiments were carried out at the BW5 experimental station at HASYLAB, DESY in Hamburg, Germany. All the samples were examined in transmission geometry. The energy of synchrotron radiation was 98.9 keV. Scattered intensity was measured between 0.5 and 19E^{-1} . Raw data were corrected for detector dead-time, polarization, absorption and variation in detector solid angle [13]. The scattering intensity was converted into the coherent scattering intensity per atom in electronic units by using the Krogh-Moe-Norman method [14, 15]. Compton scattering was corrected using the values given by Balyuzi [16]. Faber-Ziman [17] total structure factor $S(Q)$ was calculated from the scattering intensity as

$$S(Q) = \frac{I_{e.u.}^{coh}(Q) - \left\{ \langle f^2(Q) \rangle - \langle f(Q) \rangle^2 \right\}}{\langle f(Q) \rangle^2} \quad (1)$$

with

$$\langle f(Q) \rangle^2 = \sum_i c_i f_i^2(Q), \quad \langle f(Q) \rangle = \sum_i c_i f_i(Q), \quad (2)$$

where c_i is the molar fraction and $f_i(Q)$ is the total atomic scattering factor of the i -th component of the glass.

The total pair distribution function $g(r)$ was obtained via transformation

$$g(r) = 1 + \frac{1}{2\pi^2 r \rho_0} \int_0^\infty Q [S(Q) - 1] \sin(Qr) dQ, \quad (3)$$

where ρ_0 is the average number density.

It is known that the impact of chalcogenide glasses induced by external influence (i.e. γ -irradiation, hydrostatic pressure or illumination) on the experimental structure factors is rather small [4, 18–21]. Therefore, the experimental error should be minimized for correct investigation of such phenomena. In the present study, like in the case of $\text{Ge}_x\text{Sb}_{40-x}\text{S}_{60}$ glasses [18], all XRD experiments were carried out within a couple of hours; the specimens were of the same thickness; they were fixed in a holder moving horizontally, providing practically identical sample adjustment during measurements. The samples were positioned in the holder at the same position to be measured first as γ -irradiated and then as annealed after γ -irradiation. All this helped to reduce the random error to a minimum.

3. Results

Experimental structure factors $S(Q)$ for the investigated $\text{Ge}_x\text{As}_{40-x}\text{S}_{60}$ glasses in γ -irradiated and annealed after γ -irradiation states are shown in Fig. 1a. Oscillations in $S(Q)$ persist up to high Q values for all the samples. The first sharp diffraction peak (FSDP) exists on the $S(Q)$ for all the alloys studied (Fig. 1b). The intensity of the FSDP, measured as a relation of the intensities at the maximum and at the tail of peak ($I_{\text{FSDP}} = S(Q)_{\text{max}}/S(Q)_{\text{min}}$), for the annealed samples demonstrates non-monotonic trend from 4.38 at $x=16$ to 4.06 at $x=36$ reaching a maximum value of 4.56 at $x=32$. Position of the FSDP shifts continuously from 1.13E^{-1} ($x=16$) to 1.01\AA^{-1} ($x=36$). It should be noted that the values of $Q_{\text{FSDP}} = 1.08\text{\AA}^{-1}$ and 1.01\AA^{-1} for $x=24$ and 36 of the $\text{Ge}_x\text{Sb}_{40-x}\text{S}_{60}$ glasses agree with the values of $Q_{\text{FSDP}} = 1.08\text{E}^{-1}$ and 1.02E^{-1} for $x=25$ and 35 of $\text{Ge}_x\text{Sb}_{40-x}\text{S}_{60}$ glasses [18]. This non-monotonic trend in the FSDP intensity and monotonic one in the FSDP position detected for the annealed $\text{Ge}_x\text{As}_{40-x}\text{S}_{60}$ glasses have also been observed in other non-stoichiometric $\text{Ge}_x\text{As}_x\text{S}_{100-2x}$ and $\text{Ge}_x\text{As}_y\text{S}_{100-x-y}$ glasses in the course of neutron and X-ray diffraction studies [22, 23].

For all the compositions studied, positions of maxima and minima of the structure factors of γ -irradiated and annealed glasses coincide with those of radiation-modified $\text{Ge}_{25}\text{Sb}_{15}\text{S}_{60}$ and $\text{Ge}_{35}\text{Sb}_5\text{S}_{60}$ glasses. Main difference between γ -irradiated and annealed glasses is observed only in the intensity of the FSDP for As-enriched composition $\text{Ge}_{16}\text{As}_{24}\text{S}_{60}$ for which the pre-peak becomes weaker and broader under irradiation (Fig. 1b) similarly to the binary As_2S_3 glass [19]. This

difference is notably larger than the total experimental error of the structure factor, which is estimated to be below 1% in the low Q -part of $S(Q)$ as shown in [18].

Fig. 2a shows the pair distribution functions $g(r)$ for the investigated $\text{Ge}_x\text{As}_{40-x}\text{S}_{60}$ glasses, both in the γ -irradiated and annealed after γ -irradiation states. For a better comparison, parts of the pair distribution functions

$g(r)$ corresponding to the first and second (insertion) coordination shells are plotted in Fig. 2b. For all the alloys studied, a peak on $g(r)$ at $r = 2.26\text{-}2.27 \text{ \AA}$ can be attributed to the nearest neighbor correlations. On the pair distribution functions of $\text{Ge}_x\text{As}_{40-x}\text{S}_{60}$, there is either a small peak (for $x = 16$ and 24) or a shoulder (for $x = 32$ and 36) at $r \approx 2.60\text{-}2.65 \text{ \AA}$. As this distance does

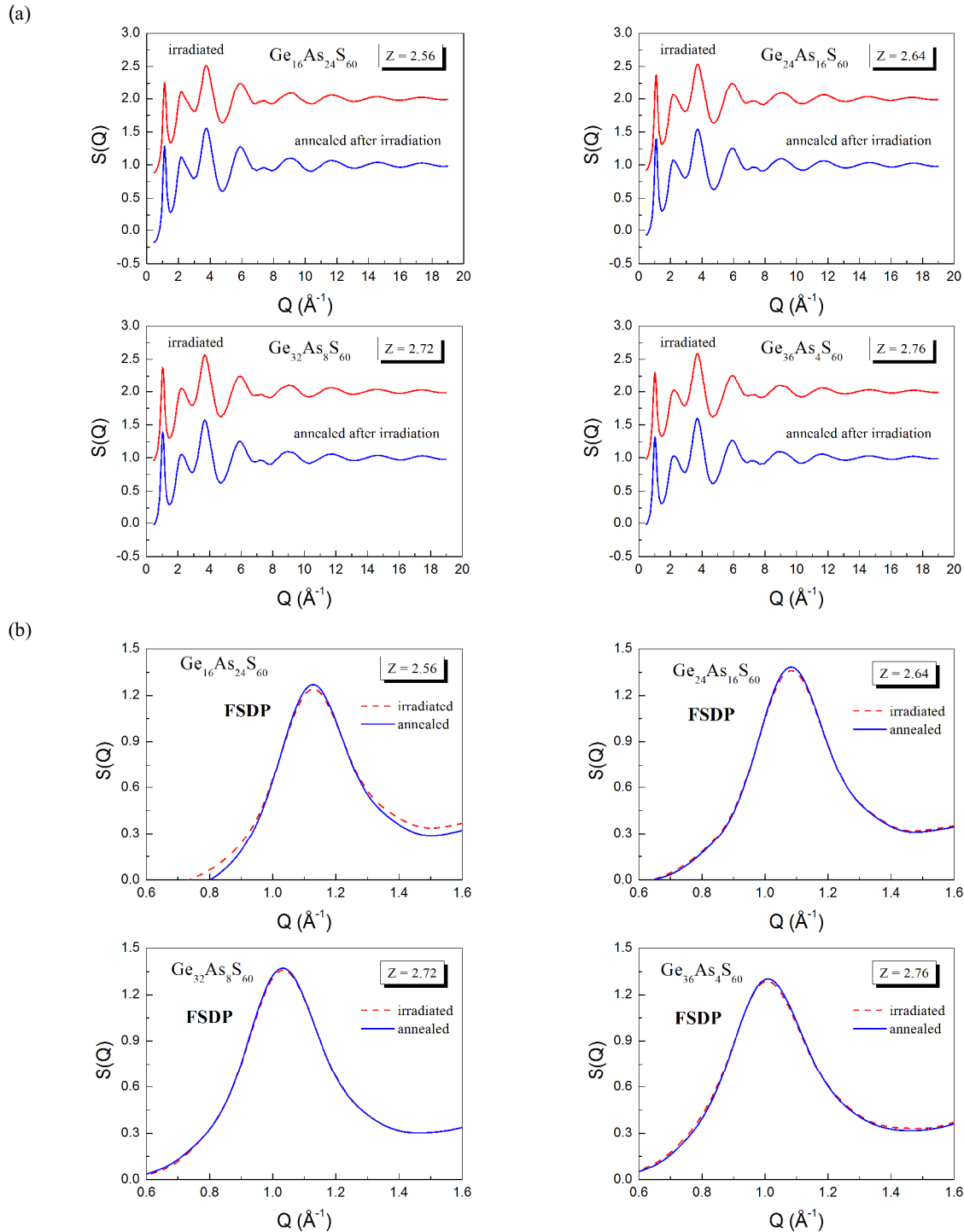


Fig. 1. (a) The total structure factors $S(Q)$ for the samples of the investigated $\text{Ge}_x\text{As}_{40-x}\text{S}_{60}$ system in γ -irradiated (the curves for γ -irradiated state is shifted (+1) for clarity) and annealed after γ -irradiation states; and (b) the first sharp diffraction peak (FSDP) in γ -irradiated and annealed after γ -irradiation states.

not correlate with any possible interatomic distance of any two glass constituents, most probably this feature (peak, shoulder) is caused by the termination of the experimental data at a final value of the diffraction vector. It is known that false oscillations appear on the pair distribution function near the main peak due to the termination effect [24]. A maximum at $r = 3.55\text{-}3.60 \text{ \AA}$

reflects the second coordination sphere. Also, a hump at $r = 2.99 \text{ \AA}$ is observed on $g(r)$ of all the investigated samples in the second coordination shell like to the samples of $\text{Ge}_x\text{Sb}_{40-x}\text{S}_{60}$ with $x = 25$ and 35 [18]. But due to the risk that this hump may come from the termination effect, we will not analyze this hump in further consideration.

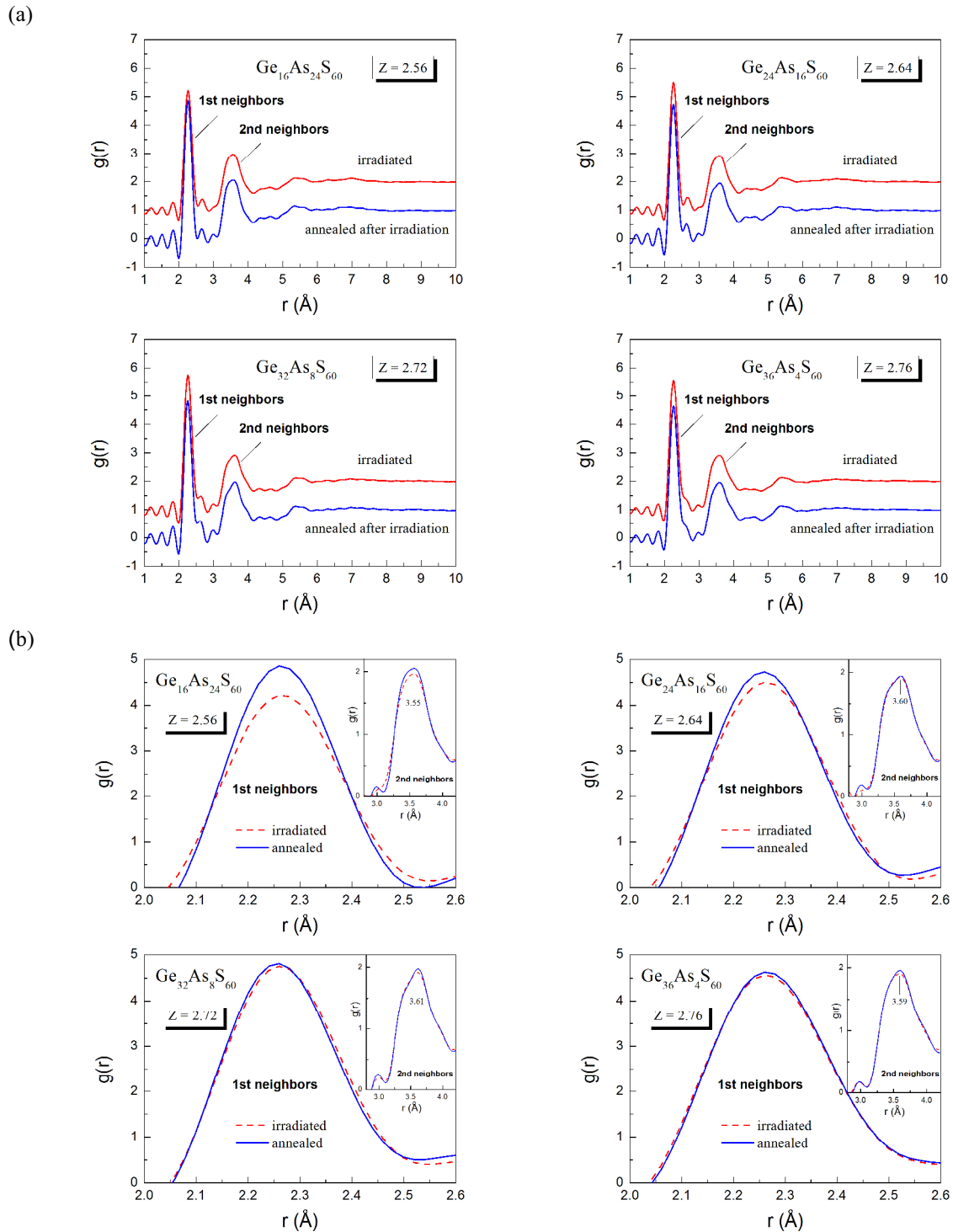


Fig. 2. (a) The pair distribution functions $g(r)$ for the samples of the investigated $\text{Ge}_x\text{As}_{40-x}\text{S}_{60}$ system in γ -irradiated (the curves for γ -irradiated state is shifted (+1) for clarity) and annealed after γ -irradiation states; and (b) the part of $g(r)$ in the first and second (insertion) coordination shells in γ -irradiated and annealed after γ -irradiation states.

Fig. 3 shows the observed peaks on $g(r)$ located in the first and second coordination shells for the annealed samples of $\text{Ge}_x\text{As}_{40-x}\text{S}_{60}$ system. One may clearly see that the first peak at $r = 2.26\text{-}2.27 \text{ \AA}$ becomes weaker and broader with increasing x . The second peak $r = 3.55\text{-}3.60 \text{ \AA}$ becomes weaker and broader with increasing x similar to the first peak. The shape of the second peak is different for the As-rich sample ($x_{\text{Ge}} = 16$) as compared to the Ge-rich samples ($x_{\text{Ge}} = 24, 32$ and 36), which have slightly narrower maximum.

The structural parameters such as intensity and position of the FSDP, as well as intensities and positions of the peaks $g(r_1)$ and $g(r_2)$ for $\text{Ge}_x\text{As}_{40-x}\text{S}_{60}$ glasses are given in Table. The intensities of these structural parameters are also plotted in Fig. 4 as a function of x for better observation of their compositional dependence. The plots of the I_{FSDP} , $g(r_1)$ and $g(r_2)$ as a function of x for both irradiated and annealed samples show non-monotonic trend with an extremum at $x = 32$.

Finally, for all the glasses studied, it is found that radiation impact results in weakening and broadening of the FSDP with the first peak at $r = 2.26\text{-}2.27 \text{ \AA}$ and the second peak at $r = 3.55\text{-}3.60 \text{ \AA}$; the effect is the largest one for $\text{Ge}_{16}\text{As}_{24}\text{S}_{60}$ ($x = 16$), smaller for $\text{Ge}_{24}\text{As}_{16}\text{S}_{60}$ ($x = 24$), and practically invisible for $\text{Ge}_{32}\text{As}_8\text{S}_{60}$ ($x = 32$) and $\text{Ge}_{36}\text{As}_4\text{S}_{60}$ ($x = 36$) alloys.

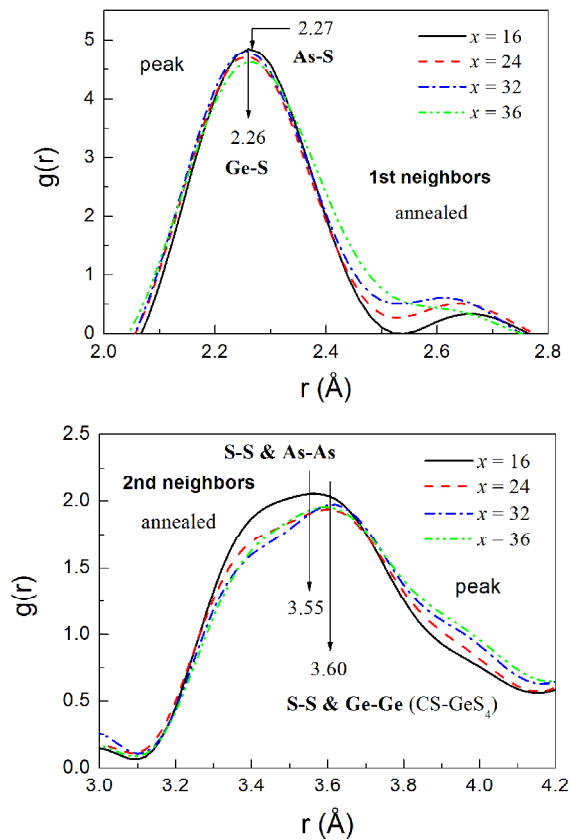


Fig. 3. The observed peaks on $g(r)$ located in the first and second coordination shells for the annealed samples of $\text{Ge}_x\text{As}_{40-x}\text{S}_{60}$ system. See the text for details.

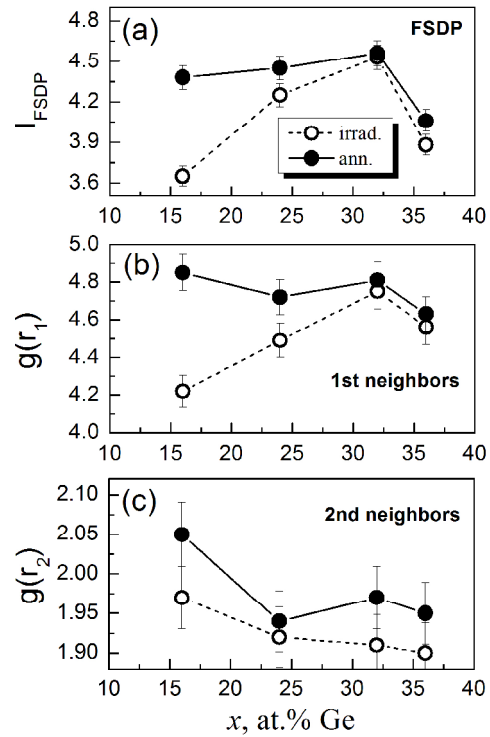


Fig. 4. The intensities of the peaks (a) FSDP, measured as a ratio of the intensities at the maximum and at the tail of peak ($I_{\text{FSDP}} = S(Q)_{\text{max}}/S(Q)_{\text{min}}$), (b) $g(r_1)$, and (c) $g(r_2)$ for the investigated $\text{Ge}_x\text{As}_{40-x}\text{S}_{60}$ glasses in γ -irradiated (open cycles) and annealed after γ -irradiation (closed cycles) states as a function of the composition x .

4. Discussion

Investigating the physical properties, in particular, optical band gap E_g and structural compactness δ in the bulk glasses and thin films from $\text{Ge}_x\text{As}_{40-x}\text{S}_{60}$ family in dependence on x or average coordination number Z (i.e., $Z = (4x + 3(40-x) + 2 \cdot 60)/100$, where 4, 3 and 2 stand for the coordination numbers of Ge, As, and S, respectively), Skordeva and Arsova [25] concluded that the peculiarities of the properties (e.g., a maximum on E_g for annealed films and a minimum on δ for bulk glasses) are caused by the topological structural 2D-3D phase transition according to the Tanaka model [26] from a two-dimensional (2D) layer-like structure to a three-dimensional (3D) cross-linked network at the average coordination number Z of about 2.67. Later Tichy and Ticha [27] reported on the possibility of chemical threshold at $Z \sim 2.7$.

Stronski *et al.* [28] reported that the compactness δ is well sensitive to the structure of glass network and its compositional dependence is supposed to be connected with atomic rearrangements in the glass backbone. On the other hand, in the first approximation, the compactness δ is also a measure of free volume of glass [29]. It is interesting to note that the compactness δ for

Table. Structural parameters of $\text{Ge}_x\text{As}_{40-x}\text{S}_{60}$ glasses ($x = 16$ ($Z = 2.56$), $x = 24$ ($Z = 2.64$), $x = 32$ ($Z = 2.72$), and $x = 36$ ($Z = 2.76$)) in γ -irradiated (irrad.) and annealed after γ -irradiation (ann.) states. Q_{FSDP} – position of the FSDP and I_{FSDP} – intensity of the FSDP, measured as a relation of the intensities at the maximum and at the tail of peak ($I_{\text{FSDP}} = S(Q)_{\text{max}}/S(Q)_{\text{min}}$); r_i – position and $g(r_i)$ – intensity of peaks on the pair distribution functions. The errors of Q_{FSDP} and r_i are estimated from the Gaussian fits of the peaks. The error bars for the I_{FSDP} and $g(r_i)$ are $\pm 2\%$ of the reported values.

x	State	$Q_{\text{FSDP}} (\text{\AA}^{-1})$	I_{FSDP} (a.u.)	$r_1 (\text{\AA})$	$g(r_1)$	$r_2 (\text{\AA})$	$g(r_2)$
16	irrad.	1.13 \pm 0.01	3.65 \pm 0.07	2.27 \pm 0.01	4.22 \pm 0.08	3.55 \pm 0.02	1.97 \pm 0.04
	ann.	1.13 \pm 0.01	4.38 \pm 0.09	2.27 \pm 0.01	4.85 \pm 0.10	3.55 \pm 0.02	2.05 \pm 0.04
24	irrad.	1.08 \pm 0.01	4.25 \pm 0.09	2.26 \pm 0.01	4.49 \pm 0.09	3.60 \pm 0.02	1.92 \pm 0.04
	ann.	1.08 \pm 0.01	4.45 \pm 0.09	2.26 \pm 0.01	4.72 \pm 0.09	3.60 \pm 0.02	1.94 \pm 0.04
32	irrad.	1.03 \pm 0.01	4.53 \pm 0.09	2.26 \pm 0.01	4.75 \pm 0.10	3.61 \pm 0.02	1.91 \pm 0.04
	ann.	1.03 \pm 0.01	4.56 \pm 0.09	2.26 \pm 0.01	4.81 \pm 0.10	3.61 \pm 0.02	1.97 \pm 0.04
36	irrad.	1.01 \pm 0.01	3.88 \pm 0.08	2.26 \pm 0.01	4.56 \pm 0.09	3.59 \pm 0.02	1.90 \pm 0.04
	ann.	1.01 \pm 0.01	4.06 \pm 0.08	2.26 \pm 0.01	4.63 \pm 0.09	3.59 \pm 0.02	1.95 \pm 0.04

the $\text{Ge}_x\text{As}_{40-x}\text{S}_{60}$ glasses has attained a minimum value at $Z = 2.72$ (see Fig. 3 in [13]). Thus, the maximum free volume in the investigated $\text{Ge}_x\text{As}_{40-x}\text{S}_{60}$ glasses is attained for alloy with $x = 32$ ($Z = 2.72$). Hence, it is reasonable to relate the features (plateau, extremum) observed in the composition trends of the FSDP intensity and those of the peaks $g(r_1)$ and $g(r_2)$ for alloy with $x = 32$ ($Z = 2.72$) with the maximum free volume and atomic rearrangements resulting in the topological or chemical threshold attained at $Z \sim 2.7$ (Fig. 4). These findings may be considered as an evidence of the anomalous structural features on the short-range order (exemplified by the first and second neighbor correlations) and medium-range order (exemplified by the FSDP) scale in the vicinity of the topological or chemical threshold at $Z \sim 2.7$.

Let us consider the radiation/annealing-induced structural changes detected on the FSDP and the pair distribution functions $g(r)$ for the investigated glasses (Figs. 1, 2, 4 and Table).

The well observable weakening and broadening of the FSDP with the unchanged position under irradiation for the As-enriched glass $\text{Ge}_{16}\text{As}_{24}\text{S}_{60}$ ($x = 16$) is similar to the radiation-induced changes [20] and photo-induced changes [4] in the FSDP intensity and position for the binary As_2S_3 glass. Thus, the mechanism of the radiation- and photo-induced structural changes on the medium-range order scale exemplified by the FSDP would be the same.

As it was mentioned in Introduction, according to the Tanaka model [4], the photo-structural changes on the medium-range order scale may be considered as a signature of photo-induced defect formation with the density less than 1% (i.e., one photo-induced atomic site per cube with a side length of 5-6 atoms). Thus, the

radiation-induced changes observed on the medium-range order scale (FSDP) indicate formation of one radiation-induced atomic site per cube with a side length of 5-6 atoms (1-3 nm). According to the Tanaka model [4], with account of the term for the single radiation-induced atomic site (defect), we consider a strain produced by γ -irradiation and confined in the cube leading finally to a radiation-induced metastable structural configuration, which can then relax into a stable structure with thermal relaxation induced by annealing (reversible changes). Producing the strain in chalcogenide glass matrix under γ -irradiation is confirmed by the recent study of microindentation cracks in bismuth-doped arsenic selenide glasses [30]. In particular, it has been found that radial cracks around indentations are produced on the surfaces of the chalcogenide glass samples at loads exceeding the specific applied load P_c^{app} that somewhat increases under γ -irradiation of samples even at the relatively low 0.76 MGy accumulated dose. Besides, the well known increase in microhardness of chalcogenide glass under γ -irradiation may also be an additional confirmation for this ([31] and references therein).

The mechanism providing formation of radiation-induced strain can be considered using both defect models and non-defect or distortion model reported by Tanaka [4] to explain the photo-structural changes in As_2S_3 chalcogenide glass and similar materials. Although different known structural models could be applied to interpret the observed weakening and broadening of the FSDP under γ -irradiation (Fig. 1b), we prefer more Tanaka's explanation of the weakening and broadening of the FSDP on illumination within the distortion model ([4] and references therein). In this approach, there are two kinds of the structural changes

involved in this model. On the one hand, plausible structural changes can be sought in the distortions in bond angles, dihedral angles, and van der Waals distances resulting in: (i) changes in the short-range order, (ii) the increase in the conduction band width and, consequently, decrease in the optical band gap (darkening effect), and (iii) the enhancement of the randomness in the medium-range structural order. On the other hand, the intermolecular distortion through bond-twisting motion of chalcogen atom is the second kind of the structural changes within the distortion model. Finally, according to the Tanaka model [4], these two kinds of structural changes are interrelated (thus, if an intermolecular bond is distorted on illumination, structural relaxation will necessarily occur, leading to appreciable angular distortions) and appear to be consistent with the weakening and broadening of the FSDP on illumination.

With account of the above mentioned, we suggest that the observed radiation-induced structural changes on the medium-range order scale (FSDP) in $\text{Ge}_{16}\text{As}_{24}\text{S}_{60}$ ($x = 16$) glass are caused by distortion in bond angles, dihedral angles, van der Waals distances and intermolecular distortion through bond-twisting motion of chalcogen atom leading together to formation of radiation-induced defects with the density $\sim 1\%$ ($\sim 10^{20} \text{ cm}^{-3}$), which annihilate with annealing through thermal relaxation of the radiation-induced metastable structural configuration (strain) to a more stable structure. As the changes in the FSDP are very small for $\text{Ge}_{24}\text{As}_{16}\text{S}_{60}$ ($x = 24$) and invisible for $\text{Ge}_{32}\text{As}_8\text{S}_{60}$ ($x = 32$) and $\text{Ge}_{36}\text{As}_4\text{S}_{60}$ ($x = 36$), one may assume that the radiation-induced defects with the density $\sim 1\%$ are probably not formed for the Ge-enriched glasses studied with dominant Ge–S correlations. In other words, we may conclude that the radiation/annealing-induced structural changes on the medium-range order scale for the $\text{Ge}_x\text{As}_{40-x}\text{S}_{60}$ system occur mainly in the As–S sub-system.

The distortion model seems to be applicable for the interpretation of the radiation/annealing-induced structural changes on the short-range order scale exemplified by the first and second coordination shells on the pair distribution functions $g(r)$ as well. Let us consider this in detail.

The first peaks on $g(r)$ at 2.26 and 2.27 Å for the $\text{Ge}_x\text{As}_{40-x}\text{S}_{60}$ glasses can be attributed to the Ge–S and As–S correlations. The value 2.26 Å for Ge-enriched samples ($x = 24, 32, \text{ and } 36$) is consistent with 2.21–2.24 Å distances corresponding to Ge–S first neighbors in the germanium sulphide glasses [32] and with 2.24–2.27 Å distances corresponding to Ge–S first neighbors in the mixed germanium-arsenic sulphide glasses [23, 24], as well as the value 2.27 Å for As-enriched sample ($x = 16$) is consistent with 2.27–2.30 Å distances corresponding to As–S first neighbors in the arsenic trisulphide glass [20, 33–35] and with 2.17–

2.27 Å distances corresponding to As–S first neighbors in the mixed Ge–As sulphide glasses [23, 24].

As–As (2.43–2.53 Å [23, 24, 32]), Ge–Ge (2.46 Å [36]) and S–S (2.0–2.04 Å [23, 32]) neighbor correlations (if exist) cannot be resolved on the pair distribution functions as they can simply be covered by the peak from Ge–S or As–S contributions. Besides, like for $\text{Ge}_x\text{Sb}_{40-x}\text{S}_{60}$ [19], we suppose that S–S bonds are very improbable in the $\text{Ge}_x\text{As}_{40-x}\text{S}_{60}$ glasses.

It is difficult to resolve the peak located at 3.55–3.6 Å on the pair distribution functions $g(r)$. In $\text{Ge}_x\text{Sb}_{40-x}\text{S}_{60}$ family, Kakinuma *et al.* [37] attributed the peak at 3.61 Å to the secondary partial correlations Ge–Ge, Ge–Sb, Sb–Sb, and S–S. The structural study of Ge–S glasses [32] shows that the broad peak at ~ 3.6 Å corresponds to the second S–S and Ge–Ge correlations in the corner-shared GeS_4 tetrahedra (CS–GeS_4). The structural study of As_2S_3 glass [20, 33–36] indicates that the broad peak at ~ 3.5 Å corresponds to the second neighbor distances S–S and As–As in the corner-shared AsS_3 pyramids. Brabec [33] reported that in As_2S_3 glass the As–As second-neighbor distance is 3.52 ± 0.01 Å and the S–S second-neighbor distance is 3.5 ± 0.1 Å. Soyer-Uzun *et al.* [23, 24] showed that for the $\text{Ge}_x\text{As}_y\text{S}_{100-2x}$ glasses a peak centered at ~ 3.4 Å can be readily correlated to the metal-metal next-nearest neighbors that are connected through S atom, namely Ge–S–Ge, Ge–S–As, and As–S–As linkages, as well as a peak centered at ~ 3.5 Å for the $\text{Ge}_x\text{As}_y\text{S}_{100-x-y}$ glasses corresponds primarily to As–As and Ge–Ge/As next-nearest neighbors in the As–S–As and Ge–S–Ge/As linkages. In principle, all secondary partial correlations Ge–Ge, Ge–As, As–As and S–S may exist in $\text{Ge}_x\text{As}_{40-x}\text{S}_{60}$ family within the range of 3.5–3.6 Å distances. Taking into account different shapes of the second peak on $g(r)$ at $r = 3.55$ Å (for $x = 16$) and $r = 3.6$ Å (for $x = 24, 32, 36$) in Fig. 3, it is reasonable to separate secondary partial correlations S–S and As–As for As-enriched sample ($x = 16$) and S–S and Ge–Ge for Ge-enriched samples ($x = 24, 32, 36$).

Similar to the $\text{Ge}_x\text{Sb}_{40-x}\text{S}_{60}$ glasses [19, 37], the intensity of the second peak $g(r_2)$ for Ge-enriched samples increases, and its position r_2 shifts to lower r values with increasing the Ge concentration with maximum for $\text{Ge}_{32}\text{As}_8\text{S}_{60}$ glass (Table). The ratio of the peak positions at 3.6 Å (second neighbor correlations) and 2.26 Å (first neighbor correlations) is 1.59. This is somewhat lower than the value of $\sqrt{8/3} = 1.63$ for perfect tetrahedra, what can be a result of $\text{GeS}_{4/2}$ unit deformation, probably, due to the existence of Ge–Ge bonding in the ethane-like units $\text{S}_{3/2}\text{Ge–GeS}_{3/2}$ ($\text{Ge}_2\text{S}_{6/2}$) in non-stoichiometric alloys of $\text{Ge}_x\text{As}_{40-x}\text{S}_{60}$

or $\text{As}_2\text{S}_3 - \text{Ge}_2\text{S}_3$ family [38]. Recently, the existence of the ethane-like units $\text{S}_{3/2}\text{Ge} - \text{GeS}_{3/2}$ has also been confirmed for the technologically important multicomponent $\text{GeS}_2 - \text{In}_2\text{S}_3 - \text{AgI}$ chalcogenide glasses [39] by using combination of XRD, EXAFS, reverse Monte Carlo modelling, Raman scattering and density functional theoretical calculations [40].

It is noteworthy that the radiation/annealing-induced changes in the main peak $g(r_1)$ correlate well with those for the FSDP (see Figs 1b, 2b and 4), i.e., the first peak $g(r_1)$ reveals the largest changes (weakening and broadening) under γ -irradiation mainly for As-enriched $\text{Ge}_{16}\text{As}_{24}\text{S}_{60}$ ($x = 16$) alloy, smaller changes for $\text{Ge}_{24}\text{As}_{16}\text{S}_{60}$ ($x = 24$) and practically no changes for $\text{Ge}_{32}\text{As}_8\text{S}_{60}$ ($x = 32$) and $\text{Ge}_{36}\text{As}_4\text{S}_{60}$ ($x = 36$) compounds. The second peak $g(r_2)$ exhibits the largest effect (weakening and broadening) under γ -irradiation for As-enriched $\text{Ge}_{16}\text{As}_{24}\text{S}_{60}$ ($x = 16$) glass as well. Thus, we assume like to the medium-range order (FSDP) that the radiation/annealing-induced structural changes on the short-range order scale (first and second coordination shells) are plausibly connected with the structural transformations in the As-S sub-system. Tanaka's approach within the distortion model explains also weakening and broadening of the first and second peaks on $g(r)$ under irradiation due to intermolecular distortion through bond-twisting motion of chalcogen atom, which is also interrelated with the distortion in bond angles, dihedral angles, and van der Waals distances.

It should be noted that the recent [41] Doppler broadening spectroscopy study of $(\text{As}_2\text{S}_3)_x(\text{GeS}_2)_{1-x}$ glasses (As_2S_3 ($x = 1.0$), $\text{Ge}_{9.5}\text{As}_{28.6}\text{S}_{61.9}$ ($x = 0.6$), $\text{Ge}_{15.8}\text{As}_{21}\text{S}_{63.2}$ ($x = 0.4$), and $\text{Ge}_{23.5}\text{As}_{11.8}\text{S}_{64.7}$ ($x = 0.2$)) in the unirradiated (annealed) and γ -irradiated states showed that the defect structure of $\text{Ge}_{15.8}\text{As}_{21}\text{S}_{63.2}$ glass is significantly different as compared to other alloys (obviously, as a result of different mechanisms (defect or non-defect ones) of radiation-structural changes). Kavetsky *et al.* [42] reported that the charged coordination topological defects are quite responsible for the defect mechanism of radiation-structural changes in the case of $\text{Ge}_{15.8}\text{As}_{21}\text{S}_{63.2}$ glass. While, likely to photo-structural changes, the non-defect mechanism within the Tanaka distortion model is supposed to be responsible for the radiation-structural changes in the As_2S_3 alloy and similar materials. The void-species nanostructure (nanovoids) of the As_2S_3 -based glasses studied with positron annihilation lifetime spectroscopy [43] should be taken into account for further consideration of validity of Tanaka's distortion model in explanation of radiation-structural changes in chalcogenides.

In summary, with account of the results obtained, we speculate that the existence of the focal point (~ 2.0 MGy) for the investigated $\text{Ge}_x\text{As}_{40-x}\text{S}_{60}$ glasses, at which the γ -irradiation-induced optical (darkening) effect does not depend on the composition [11], can simply be related with the dominant radiation-structural

changes in the As-S sub-system, and embedding the Ge atoms into As-S glass matrix does not affect their mechanism, since the radiation-structural changes in the Ge-S sub-system are invisible on both short- and medium-range order scales. Finally, we would like to state that the alternative interpretation of the radiation/annealing-induced structural changes reported here may be also proposed.

5. Conclusions

Impact of γ -irradiation (2.41 MGy dose) and subsequent annealing on the atomic structure of $\text{Ge}_x\text{As}_{40-x}\text{S}_{60}$ glasses ($x = 16, 24, 32, 36$) is studied using high-energy XRD measurements. Analysis of the experimental structure factors and pair distribution functions has revealed the differences related to the structural changes at the short-range order scale (exemplified by the first and second nearest neighbor correlations) and medium-range order scale (exemplified by the FSDP). Nonlinear compositional trends in the I_{FSDP} , $g(r_1)$ and $g(r_2)$ values with features (plateau, extremum) nearby the topological structural phase transition [26] or chemical threshold [27] at the average coordination number $Z \sim 2.7$ ($x = 32$) are detected for the both γ -irradiated and annealed alloys.

The FSDP position is found to be constant on radiation/annealing treatment, but the intensity of the FSDP reveals changes under irradiation/annealing only for the compositions with $x = 16$ and 24. The radiation/annealing-induced changes are also observed on the pair distribution functions in the first and second coordination shells for these compounds. Practically invisible effects on the FSDP and pair distribution functions are found for the alloys with $x = 32$ and 36. The radiation/annealing-induced structural changes detected mainly in the As-S sub-system of the glasses examined can be well explained within the Tanaka approach [4] for interpretation of the photo-induced structural changes and related phenomena in the As_2S_3 chalcogenide glass and similar materials.

Existence of the focal point (~ 2.0 MGy) for the $\text{Ge}_x\text{As}_{40-x}\text{S}_{60}$ glasses, at which the γ -irradiation-induced optical (darkening) effect does not depend on the composition [11], can simply be related with the dominant radiation-structural changes in the As-S sub-system and embedding the Ge atoms into the As-S glass matrix does not affect their mechanism, since the radiation-structural changes in the Ge-S sub-system are invisible on both short- and medium-range order scales.

Acknowledgements

The authors would like to thank Dr. Ivan Kaban (IFW Dresden, Germany) for his help with high-energy synchrotron XRD measurements, Dr. Pal J3v3ari

(Research Institute for Solid State Physics and Optics, Budapest, Hungary) for his help with experimental data treatment, Prof. Walter Hoyer (Institute of Physics, TU Chemnitz, Germany) and Prof. Guorong Chen (East China University of Science and Technology, Shanghai, China) for stimulating discussions. The investigated samples used for measurements were prepared within joint research projects (#0106U007386 and #0109U007446c) between Ivan Franko Drohobych State Pedagogical University (Drohobych, Ukraine) and Scientific Research Company “Carat” (Lviv, Ukraine) supported by the Ministry of Education and Science of Ukraine (#0106U007385 and #0109U007445). T.S.K. acknowledges DAAD for support of his research work at TU Chemnitz (Germany) and Deutsches Elektronen-Synchrotron DESY for support of the experiments performed at HASYLAB (Hamburg, Germany). T.S.K. and V.M.T. acknowledge national project (#0111U001021) supported by the Ministry of Education and Science, Youth and Sport of Ukraine. A.L.S. grateful to the Alexander von Humboldt Foundation, DFG and DAAD (Germany). Support from the Ukrainian-Russian projects funded by the State Fund for Fundamental Researches of Ukraine (#F40.2/019) and the Ministry of Education and Science of the Russian Federation (#02.740.11.0797) and the Russian Foundation for Basic Research (#11-02-90420-Ukraine, #11-02-91341-Germany and #12-02-00528-a) is also gratefully acknowledged.

References

- S.A. Dembovsky, A.S. Zyubin, F.V. Grigor'ev, Modeling of hypervalent configurations, valence alternation pairs, deformed structure, and properties of a -S and a -As₂S₃ // *Semiconductors*, **32**(8), p. 843-849 (1998).
- M. Munzar, L. Tichy, Kinetics of photo-darkening and self-bleaching in amorphous As₂S₃ and As₂Se₃ thin films // *Phys. Stat. Sol. (RRL)*, **1**(2), p. R74-R76 (2007).
- K. Shimakawa, N. Yoshida, A. Ganjo, Y. Kuzukawa, J. Singh, A model for the photostructural changes in amorphous chalcogenides // *Philos. Mag. Lett.*, **77**(3), p. 153-158 (1998).
- K. Tanaka, Photoinduced structural changes in amorphous semiconductors // *Semiconductors*, **32**(8), p. 861-866 (1998).
- K. Shimakawa, A. Kolobov, S.R. Elliott, Photoinduced effects and metastability in amorphous semiconductors and insulators // *Adv. Phys.*, **44**(6), p. 475-588 (1995).
- T.S. Kavetskiy, Impact of the sample thickness and γ -irradiation dose on the occurrence of radiation-induced optical effects in chalcogenide vitreous semiconductors of the Ge-Sb-S system // *Semiconductors*, **45**(4), p. 499-502 (2011).
- O.I. Shpotyuk, R.Ya. Golovchak, A.P. Kovalskiy, T.S. Kavetskiy, Time and temperature stability of radiation-induced changes of optical properties in ternary systems of chalcogenide vitreous semiconductors // *Functional Materials*, **10**(2), p. 317-321 (2003).
- O.I. Shpotyuk, T.S. Kavetskiy, A.P. Kovalskiy, V. Pamukchieva, Gamma-irradiation effect on the optical properties of Ge_xSb_{40-x}S₆₀ chalcogenide glasses // *Proc. SPIE*, **4415**, p. 278-283 (2001).
- O. Shpotyuk, A. Kovalskiy, T. Kavetskiy, R. Golovchak, Post-irradiation thermally stimulated recovering effects in some ternary chalcogenide glasses // *J. Optoelectron. Adv. Mater.*, **5**(5), p. 1169-1179 (2003).
- O.I. Shpotyuk, A.P. Kovalskiy, T.S. Kavetskiy, R.Ya. Golovchak, Threshold restoration effects in γ -irradiated chalcogenide glasses // *J. Non-Cryst. Solids*, **351**, p. 993-997 (2005).
- V. Balitska, R. Golovchak, A. Kovalskiy, E. Skordeva, O.I. Shpotyuk, Effect of Co⁶⁰ γ -irradiation on the optical properties of As-Ge-S glasses // *J. Non-Cryst. Solids*, **326&327**, p. 130-134 (2003).
- A. Feltz, *Amorphous and Vitreous Inorganic Solids*. Moscow, Mir, 1986 (in Russian).
- H.F. Poulsen, J. Neufeind, H.-B. Neumann, J.R. Schneider, M.D. Zeidler, Amorphous silica studied by high energy X-ray diffraction // *J. Non-Cryst. Solids*, **188**, p. 63-74 (1995).
- J. Krogh-Moe, A method for converting experimental X-ray intensities to an absolute scale // *Acta Cryst.*, **9**, p. 951-953 (1956).
- N. Norman, The Fourier transform method for normalizing intensities // *Acta Cryst.*, **10**, p. 370-373 (1957).
- H.H.M. Balyuzi, Analytic approximation to incoherently scattered X-ray intensities // *Acta Cryst. A*, **31**, p. 600-602 (1975).
- T.E. Faber, J.M. Ziman, A theory of the electrical properties of liquid metals // *Philos. Mag.*, **11**(109), p. 153-173 (1965).
- T. Kavetskiy, O. Shpotyuk, I. Kaban, W. Hoyer, Radiation-modified structure of Ge₂₅Sb₁₅S₆₀ and Ge₃₅Sb₅S₆₀ glasses // *J. Chem. Phys.*, **128**(24), 244514(1-8) (2008).
- T. Kavetskiy, O. Shpotyuk, I. Kaban, W. Hoyer, Atomic- and void-species nanostructures in chalcogenide glasses modified by high energy gamma-irradiation // *J. Optoelectron. Adv. Mater.*, **9**(10), p. 3247-3252 (2007).
- H. Hamanaka, S. Minomura, K. Tsuji, Comparative studies of pressure and photo induced structural changes in As₂S₃ glass // *J. Non-Cryst. Solids*, **137&138**, p. 977-980 (1991).
- S.R. Elliott, Scattering studies of photostructural changes in chalcogenide glasses // *J. Non-Cryst. Solids*, **59&60**, p. 899-908 (1983).

22. S. Soyer-Uzun, S. Sen, C.J. Benmore, B.G. Aitken, Compositional variation of short- and intermediate-range structure and chemical order in Ge-As sulfide glasses: A neutron diffraction study // *J. Phys. Chem. C*, **112**, p. 7263-7269 (2008).
23. S. Soyer-Uzun, S. Sen, B.G. Aitken, Network vs molecular structural characteristics of Ge-doped arsenic sulfide glasses: A combined neutron/X-ray diffraction, extended X-ray absorption fine structure, and Raman spectroscopic study // *J. Phys. Chem. C*, **113**, p. 6231-6242 (2009).
24. R. Kaplow, S.L. Strong, B.L. Averbach, Radial density functions for liquid mercury and lead // *Phys. Rev.*, **138**, p. A1336-A1345 (1965).
25. E.R. Skordeva, D.D. Arsova, A topological phase transition in ternary chalcogenide films // *J. Non-Cryst. Solids*, **192&193**, p. 665-668 (1995).
26. K. Tanaka, Structural phase transitions in chalcogenide glasses // *Phys. Rev. B*, **39**(2), p. 1270-1279 (1989).
27. L. Tichy, H. Ticha, Is the chemical threshold in certain chalcogenide glasses responsible for the threshold at the mean coordination number of approximately 2.7? // *Phil. Mag. B*, **79**(2), p. 373-380 (1999).
28. A.V. Stronski, M. Vlček, P.F. Oleksenko, Fourier Raman spectroscopy studies of the $As_{40}S_{60-x}Se_x$ glasses // *Semiconductor Physics, Quantum Electronics & Optoelectronics*, **4**(3), p. 210-213 (2001).
29. I.P. Kotsalas, D. Papadimitriou, C. Raptis, M. Vlcek, M. Frumar, Raman study of photostructural changes in amorphous $Ge_xSb_{0.4-x}S_{0.6}$ // *J. Non-Cryst. Solids*, **226**, p. 85-91 (1998).
30. K. Sangwal, J. Borc, T. Kavetsky, Study of microindentation cracks in bismuth-doped arsenic selenide glasses // *J. Non-Cryst. Solids*, **357**, p. 3117-3122 (2011).
31. O.I. Shpotyuk, Radiation-induced effects in chalcogenide vitreous semiconductors // *Semiconducting Chalcogenide Glass I: Glass Formation, Structure, and Stimulated Transformations in Chalcogenide Glasses, Semiconductors and Semimetals*, edited by R. Fairman and B. Ushkov, Amsterdam-Boston-London-New York-Oxford-Paris-San Diego-San Francisco-Singapore-Sydney-Tokyo, Elsevier Academic Press, **78**, p. 215-260 (2004).
32. E. Bychkov, M. Miloshova, D.L. Price, C.J. Benmore, A. Lorriaux, Short, intermediate and mesoscopic range order in sulfur-rich binary glasses // *J. Non-Cryst. Solids*, **352**, p. 63-70 (2006).
33. C.J. Brabec, Structural model of amorphous arsenic sulfide // *Phys. Rev. B*, **44**(24), p. 13332-13342 (1991).
34. T.G. Fowler, S.R. Elliott, Continuous random network models for a- As_2S_3 // *J. Non-Cryst. Solids*, **92**, p. 31-50 (1987).
35. F. Shimojo, K. Hoshino, Y. Zempo, Intermediate-range order in liquid and amorphous As_2S_3 by ab initio molecular-dynamics simulations // *J. Non-Cryst. Solids*, **312-314**, p. 388-391 (2002).
36. W. Zhou, M. Pasesler, D.E. Sayers, Structure of germanium-selenium glasses: An X-ray-absorption fine-structure study // *Phys. Rev. B*, **43**(3), p. 2315-2321 (1991).
37. F. Kakinuma, T. Fukunaga, K. Suzuki, Structural study of $Ge_xSb_{40-x}S_{60}$ ($x = 10, 20$ and 30) glasses // *J. Non-Cryst. Solids*, **353**, p. 3045-3048 (2007).
38. D. Arsova, E. Skordeva, D. Nesheva, E. Vateva, A. Perakis, C. Raptis, A comparative Raman study of the local structure in $(Ge_2S_3)(As_2S_3)_{1-x}$ and $(GeS_2)(As_2S_3)_{1-x}$ glasses // *Glass Phys. Chem.*, **26**(3), p. 247-251 (2000).
39. T. Kavetsky, N. Pavlyukh, V. Tsmots, W. Wang, J. Ren, G. Chen, A.L. Stepanov, IR impurity absorption in GeS_2 - In_2S_3 - AgI chalcogenide glasses // *In book: NATO Science for Peace and Security Series B: Physics and Biophysics. Chapter 25 "Nanotechnological basis for advanced sensors"* ed. by J.P. Riethmaier, P. Paunović, W. Kulisch, C. Popov, P. Petkov, Berlin, Springer, p. 231-234 (2011).
40. A. Chrissanthopoulos, P. Jóvári, I. Kaban, S. Gruner, T. Kavetsky, J. Borc, W. Wang, J. Ren, G. Chen, S.N. Yannopoulos, Structure of AgI -doped Ge - In - S glasses: Experiment, reverse Monte Carlo modelling, and density functional calculations // *J. Solid State Chem.* (2012); <http://dx.doi.org/10.1016/j.jssc.2012.03.046>
41. T.S. Kavetsky, O. Šauša, V.F. Valeev, V.I. Nuzhdin, N.M. Lyadov, A.L. Stepanov, Raman, positron annihilation and Doppler broadening spectroscopy of gamma-irradiated and Cu-ion implanted $Ge_{15.8}As_{21}S_{63.2}$ glass // *In book: Coherent optics and optical spectroscopy: XV Intern. junior sci. school, 24-26 October 2011*. Ed. by M.Kh. Salakhov. Kazan, Kazan Univ., **15**, p. 86-89 (2011).
42. T. Kavetsky, M. Vakiv, O. Shpotyuk, Charged defects in chalcogenide vitreous semiconductors studied with combined Raman scattering and PALS methods // *Radiation Measurements*, **42**, p. 712-714 (2007).
43. T. Kavetsky, K. Kolev, V. Boev, P. Petkov, T. Petkova, A.L. Stepanov, Nanovoids in glasses and polymers probed by positron annihilation lifetime spectroscopy // *In book: NATO Science for Peace and Security Series B: Physics and Biophysics. Chapter 11 "Nanotechnological basis for advanced sensors"*, ed. by J.P. Riethmaier, P. Paunović, W. Kulisch, C. Popov, P. Petkov. Berlin, Springer, p. 103-110 (2011).